Nonlinear Dyn (2017) 88:1237–1256
DOI 10.1007/s11071-016-3307-y

ORIGINAL PAPER

On the periodic gait stability of a multi-actuated spring-mass hopper model via partial feedback linearization

Hasan Hamzaçebi · Ömer Morgül

Received: 21 April 2016 / Accepted: 19 December 2016 / Published online: 2 January 2017

Abstract Spring-loaded inverted pendulum (SLIP) template (and its various derivatives) could be considered as the mostly used and widely accepted models for describing legged locomotion. Despite their simple nature, as being a simple spring-mass model in dynamics perspective, the SLIP model and its derivatives are formulated as restricted three-body problem, whose non-integrability has been proved long before. Thus, researchers proceed with approximate analytical solutions or use partial feedback linearization when numerical integration is not preferred in their analysis. The key contributions of this paper can be divided into two parts. First, we propose a dissipative SLIP model, which we call as multi-actuated dissipative SLIP (MD-SLIP), with two extended actuators: one linear actuator attached serially to the leg spring and one rotary actuator attached to hip. The second contribution of this paper is a partial feedback linearization strategy by which we can cancel some nonlinear dynamics of the proposed model and obtain exact analytical solution for the equations of motion. This allows us to investigate stability characteristics of the hopping gait obtained from the MD-SLIP model. We illustrate the applicability of our solutions with open-loop and closed-loop hopping performances on rough terrain simulations.

H. Hamzaçebi (✉) · Ö. Morgül
Department of Electrical and Electronics Engineering, Bilkent University, 06800 Bilkent, Ankara, Turkey
e-mail: hasan@ee.bilkent.edu.tr

Ö. Morgül
e-mail: morgul@ee.bilkent.edu.tr

Keywords Spring-loaded inverted pendulum · SLIP · Legged locomotion · Hybrid dynamical system · Partial feedback linearization · Spring-mass hopper

Mathematics Subject Classification 37M99 · 68T40 · 70E60 · 70H07 · 70Q05 · 93B18

1 Introduction

One common objective of almost all robotics researchers is to build some useful machines that can serve for their interest. Actually, the exponential growth and spread of knowledge made this possible for some kind of applications such as industrial robots that replace human workers in factories for decades. However, area of legged locomotion, which aims to understand animal movements in nature and tries to build robot platforms inspired by these observations, is not as mature as the field of wheeled or tracked robotics. However, there is ample evidence, which both theoretically and practically indicates that the legged morphologies perform better than the wheeled/tracked ones, especially on rough terrains [1–3]. Therefore, the main research direction in the field of legged locomotion is to first analyze and understand legged locomotion [4,5], then build legged robots with high maneuverability and control their locomotion by inspiring from nature [6]. Detailed reviews about legged robots can be found in [7,8]

1.1 Models for running with legged robots

There are various approaches that are used to represent and study legged locomotion such as physics-based mathematical models [9,10], data-driven models [11] and central pattern generator-based models [12–14]. Among these, it would be fair to say that a vast majority of the current literature exclusively focus on developing physics-based mathematical models and performing parametric fit to the data. Note that such robot structures may have many legs and depending on their configurations, the resulting dynamical equations usually become very complex, which makes both the analysis and control of such systems extremely difficult. One way of dealing with the complexities resulting from dynamics of many-legged systems is to obtain some reduced order models, also called templates, which capture some essential features of original dynamics; see, e.g., [15]. The key reason behind this approach is that such templates and their anchors are easier to analyze and control. Since their behavior captures some essential features of the original system, the results obtained from these templates are expected to be applicable to the analysis and control of the original structure. The spring-loaded inverted pendulum (SLIP) model is one of such templates which attracted considerable attention and received wide spread acceptance in the community of biology [16,17] and robotics [1,18,19]. It has been observed both theoretically and experimentally that SLIP template, and their anchors, can successfully predict the center of mass (COM) trajectories of different animals, regardless of the number of legs; see, e.g., [2,15,20,21]. Likewise, it has also been observed that SLIP templates yield accurate ground reaction force profiles resulting in the actual motion of such legged animals; see [15,20,22]. Motivated mainly from these observations, in this work we will focus on some properties of various SLIP templates as a model to study one-legged locomotion. For more information on legged locomotion, the resulting dynamics and related subjects, the reader may resort to, e.g., [2,7], and the references therein.

Despite its simplicity, COM trajectories of SLIP model constitute a three-body problem during the phase in which the leg is in contact with the ground (stance phase) [23], and non-integrability of such systems have been shown before [24]. Having this problem in its formulation, SLIP model does not have exact analytic solutions to their stance phase dynamics. The first solution to overcome this issue is to proceed with numerical integrations, so that non-integrable nature of the system dynamics will not cause any problem. However, many robotic platforms which utilize real-time motion planning and control algorithm require solutions of the equation of motion, especially in stance phase; see, e.g., [25,26]. In such cases, the utilization of semi-analytic approximation would be much more computationally effective than the numerical integration of stance dynamics, especially in feedback control of such systems which require high performance.

Once we turn our directions to computationally efficient, analytical solutions, two main directions come forward to obtain analytic solutions to the equations of motion of the SLIP-like models. Our first choice is to utilize approximations to the non-integrable stance dynamics of the SLIP model. For this purpose, there are iterative methods in the literature that approximates the stance dynamics of a 2DOF SLIP model by using the main principles from mean value theorem [23]. Although the method is analytic by nature, its accuracy depends on the number of iterations performed during each run. Different from this method, simpler approximate analytic solutions have also been developed by assuming constant angular momentum, small angular sweep and low spring compression during the stance phase [27]. The main problem with this method comes from constant angular momentum assumption that yields high prediction performance for symmetric trajectories (see Fig. 3 for visualization of such a trajectory) that correspond to trajectories where leg length is even symmetric while leg angle is odd symmetric around the time halfway during the stance phase [1]. However, its accuracy deteriorates when the trajectory is non-symmetric [27]. Arslan et al. [9] proposed an extension to [27] in order to relieve the constant angular momentum assumption, so that the approximation holds also for the non-symmetric trajectories. The effectiveness and performance of such analytical approximate solutions have also been validated on a physical one-legged hopping robot platform [28].

Apart from using analytic approximations, partial feedback linearization also yields closed-form expressions for originally non-integrable system dynamics by eliminating some nonlinear components in the equations of motion with the help of control input. For instance, Piovan et al. [29] use a linear actuator input, connected in series with the leg spring, in order to cancel the nonlinearities in the SLIP dynamics to obtain

exact closed-form expressions. The important point here is to notice that partial feedback linearization also allows enforcing specific, analytic trajectories to the stance phase dynamics, while eliminating the nonlinearities in the system dynamics [29].

1.2 Anchoring SLIP template to MD-SLIP model

As mentioned earlier, SLIP template consists of a point mass attached to a massless leg. In order to increase its practicality, many researchers anchored to SLIP template to obtain more complex models for running with legged robots [28,30–32], whose COM trajectories can be accurately defined with SLIP template; see Sect. 1.1. This section details our extensions to SLIP template based on biological observations and engineering requirements.

Our first goal is to present a focused understanding of stability properties of hopping that are common to a wide range of legged robots. Therefore, we first extend the SLIP template with a passive, compliant damping in the leg, which is inevitable for physical robot platforms. Note that extending the SLIP template with a damping element has been utilized in the literature and its effectiveness for modeling losses in a physical robot has been shown experimentally [28].

On the other hand, existence of damping in the leg requires energy injection to the system in order to compensate for losses. Therefore, we first consider a single linear actuator, which is serial to leg spring, as in [29,33]. Physical significance of using a linear actuator in the leg has been validated in [34] by modeling muscle activation in the leg, which injects energy to legged animals during the stance phase, with a force-free leg length actuation. Note that addition of a linear actuator serial to the leg spring brings a mass to the robot leg. Various studies investigating the effect of leg mass suggest that it affects system dynamics both due to its inertia and due to the losses during the impact collisions [35]. However, effect of inertia has been found to have a minor effect on system trajectories as compared to impact collisions [35]. For the case of impact collisions, note that the linear actuator is placed between the body mass and the leg spring. Thus, linear actuator can be modeled as a part of body mass instead of leg mass. On the other hand, it has been shown that effect of leg mass during the impact collisions can be modeled with a simple inelastic collision map after the liftoff event [28]. Therefore, we neglect the mass due to the linear actuator and continue our analysis with massless leg assumption in our simulation studies. When a physical implementation is required, the inelastic collision map, which will not affect our stance dynamics solutions, can be used to consider the mass of the robot leg.

However, using a single linear actuator as in [29] limits us to enforce closed-form trajectories to either radial or angular trajectories (several equations allow enforcing constrained trajectories to radial and angular motion simultaneously [29]). Hence, we utilize a torque actuation at the hip in order to obtain analytical solutions to both radial and angular trajectory at the same time. Various studies indicate that torque-actuated SLIP model yields more accurate predictions for the ground reaction forces (GRF) as compared to basic SLIP models and their GRF responses fit better to animal locomotion data [20]. We assume fixed body orientation for torque actuation that allows the reaction force at the hip to be applied on body mass, which is assumed to be a point mass in our analysis. Note that although our assumption for fixed body orientation seems to be impractical, planarizers for legged robots make this assumption valid for template models [36]. On the other hand, a humanlike body orientation without a planarizer will need a properly chosen body angle for our desired hip torque actuation profile. However, this approach is left out of the scope of the current paper.

1.3 Contributions

In a previous work [37], we proposed an actuator enhanced SLIP model (with linear and hip actuations but without leg damping) and used a partial feedback linearization strategy to enforce analytical solutions for both radial and angular trajectories during the stance phase. After extensive simulations, our results indicated that the proposed model enlarges the stability region as compared to the original SLIP template.

The current paper first extends on our previous actuator enhanced model with a viscous damping in the leg for the sake of modeling physical losses. Although partial feedback linearization cancels damping in the equations of motion in order to obtain analytical solutions for the trajectories, we show how to deal with damping component when designing actuation input for partial feedback linearization and determining the

liftoff condition. Similar to our previous work [37], we utilize partial feedback linearization in order to enforce closed-form expressions for the radial and angular trajectories. However, different from [37], we show the applicability of the proposed method by designing a deadbeat controller based on the analytical trajectories obtained via partial feedback linearization. In addition, we investigate open-loop and closed-loop hopping performances of our model with the associated enforced closed-form solutions on different rough terrain simulations. In order to illustrate the contributions in a comparative manner, we give brief information about SLIP, TD-SLIP, active SLIP models and compare our results with these models. Finally, current work performs all the analysis in a non-dimensional coordinate system framework in order to ensure generality of our results for models with different system parameters.

1.4 Organization of the paper

This paper is organized as follows. In Section 2, background about various SLIP models, such as dissipative SLIP model, active SLIP model and torque-actuated dissipative SLIP model are reviewed. In Sect. 3, the proposed multi-actuated dissipative SLIP model and our partial feedback solution is described to obtain the closed-form solutions for its stance dynamics. In Sect. 4, stability of the periodic gaits is investigated and compared with extensive simulation studies. In Sect. 5, performance tests of the MD-SLIP model with open-loop and closed-loop controllers on rough terrain simulations are shown, and the paper is concluded in Sect. 6.

2 SLIP models

2.1 Dissipative SLIP model

The dissipative spring-loaded inverted pendulum model is an extended version of the well-known SLIP model, where a parallel damping element is added to capture dissipation behavior of the leg during the stance phase. The model consists of a body, which is assumed to be a point mass, attached to a massless leg to preserve the simplicity of the model. The leg spring has parallel compliance and damping elements as illustrated in Fig. 1.

The model has hybrid system dynamics by nature, and there are two switching sub-systems that are triggered one after another during locomotion, as illustrated in Fig. 2. First phase is called flight when the toe of the robot is on the fly and the second phase is called stance when the toe of the robot is in contact with the ground. The periodic locomotion of the robot is realized via consecutive activation of these two phases. Actually, these phases can also be divided into sub-phases of locomotion to investigate the overall behavior in detail. The flight phase have two sub-phases as *ascent* and *descent* based on the increase or decrease in the vertical position of the robot. Similarly, stance phase can be observed in two sub-phases as *compression* and *decompression*, which are discriminated as the compression and decompression behavior of the leg spring as the name refers to.

The transitions from and to the sub-phases of locomotion are described by events which are given by some predefined boundary conditions for system dynamics during associated phase of locomotion. Starting from descent phase, the robot first faces with *touchdown* event which triggers the transition from descent phase to the stance phase, where the foot gains ground contact. In the first sub-phase of stance, body mass starts

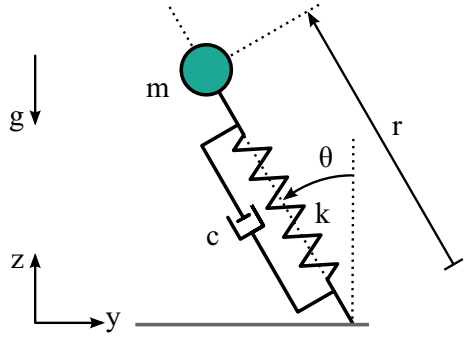

Fig. 1 Dissipative SLIP model, coordinate system and model parameters

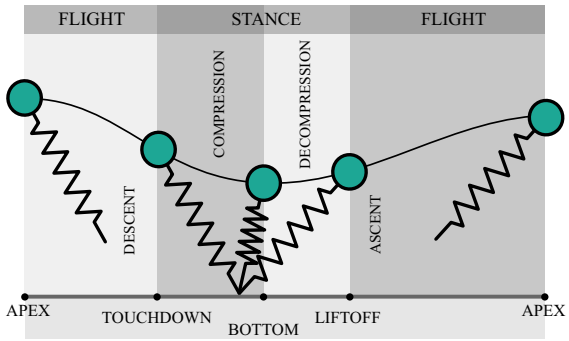

Fig. 2 Phases of locomotion

to compress the leg spring until the bottom point where the *bottom* event occurs. The *bottom* event triggers the transition from compression to decompression phase, where the body velocity changes its direction during stance and leg spring starts pushing the body upwards by using the potential energy stored in the leg spring. After some point the *liftoff* event occurs, when the toe of the robot loses the contact with the ground and robot starts to fly upwards due to the push of the leg spring. Finally, the robot reaches a maximum height where the ascent phase ends. This event is called *apex* event, which triggers the transition from ascent to descent, which will be frequently used in the paper.

In addition to various terms defined above which are utilized in the paper, at this point, we will clarify some terminology regarding the locomotion trajectory. Note that Fig. 2 represents a sample trajectory for the SLIP model. This trajectory, starting and ending at two subsequent apexes, is called a *stride*. By an abuse of notation, we will also call this motion (stride) as a gait in this paper. Obviously the concept of gait, albeit containing the motion depicted in Fig. 2, corresponds to various coordination modes of animal (or robot) legs in the literature [5,10,13]. However, one-legged template structure of the SLIP model does not allow a multi-legged gait description for one stride. On the other hand, [16] describes the locomotion performed by kangaroos as hopping gait that is also one of the locomotion types performed by using the SLIP model. Therefore, we focus on hopping gait in our analysis and we will refer to this type of locomotion as hopping gait (or simply gait) and the path it follows during the locomotion will be called trajectory throughout the paper. The locomotion of SLIP is then subsequent recursion of strides depicted in Fig. 2. A periodic motion or simply a periodic gait is such a motion where initial and final apex states are equal. The locomotion containing such periodic gaits is then called as a periodic locomotion. A periodic gait could be symmetric or asymmetric, as depicted in Fig. 3. In symmetric gaits, at the bottom event, the SLIP is vertically upwards and the resultant trajectory has the following properties; leg length is even symmetric while leg angle is odd symmetric around the bottom state [1]. Otherwise the trajectory is called asymmetric.

Our aim in this work is to analyze the existence and stability of periodic gaits of SLIP dynamics under some control laws. The main motivation behind such an aim is that such gaits could be preferred as steady-state targets in the feedback control of SLIP locomotion. Likewise, deviations from such a periodic gait could be utilized as a locomotion performance measure. In fact, if one can relate various properties of such stable periodic gaits to the control law properties, various other measures could be considered to improve the locomotion performance. For instance, a periodic locomotion could be generated by using symmetric or asymmetric gaits. While symmetric gaits are easier to analyze since they yield approximate analytical solutions, see [27], asymmetric gaits may be used to improve the stability of periodic gaits. They may be utilized to adjust foot placement, to regulate the energy or to control the horizontal position with better locomotion performance. Further information about the symmetric and asymmetric trajectories of the SLIP template can be found in [1] and the references therein.

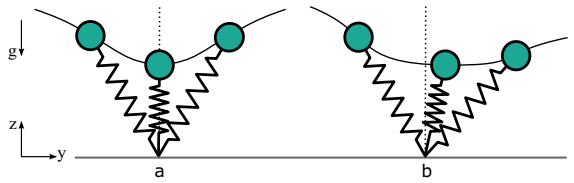

Fig. 3 A sample illustration of **a** symmetric gait and **b** asymmetric gait

In order to make sure that our analysis are parameter independent and obtain general forms, all the works in this paper will be presented with dimensionless formulation. To accomplish dimensionless quantities, time and length will be scaled with $\sqrt{r_0/g}$ and leg rest length r_0, respectively. Conversion from physical quantities to non-dimensional counterparts can be obtained by using the equations in Table 1, where variables with bars are the physical quantities of the corresponding non-dimensional parameters. Additionally, notations used for SLIP model throughout the paper are given in Table 2. Note that all relationships below use the non-dimensional parameter formulation described above unless otherwise specified.

System dynamics of the dissipative SLIP model during the flight phase is fairly simple, since the point mass follows a ballistic trajectory during its fly, which is given as

$$\ddot{y} = 0, \ddot{z} = -1 \tag{1}$$

in Cartesian coordinates.

Table 1 Dimensionless counterparts of the physical quantities

Quantity	Description
$t := \bar{t}/\sqrt{r_0/g}$	Time
$y := \bar{y}/r_0$	Length
$\dot{y} := \bar{\dot{y}}/\sqrt{gr_0}$	Velocity
$\ddot{y} := \bar{\ddot{y}}/g$	Acceleration
$\theta := \bar{\theta}$	Angle
$\dot{\theta} := \bar{\dot{\theta}}\sqrt{r_0/g}$	Angular velocity
$\ddot{\theta} := \bar{\ddot{\theta}}r_0/g$	Angular acceleration
$E := \bar{E}/(mgr_0)$	Energy
$k := \bar{k}r_0/(mg)$	Leg stiffness
$c := \bar{c}\sqrt{r_0/g}/m$	Damping constant
$\tau := \bar{\tau}/(mgr_0)$	Torque

Table 2 Notation for SLIP model used throughout the paper

SLIP parameters	
y, z	Body horizontal and vertical positions
$\dot{y}, \dot{z}$	Body horizontal and vertical velocities
$\ddot{y}, \ddot{z}$	Body horizontal and vertical accelerations
r, θ	Leg length and angle
$\dot{r}, \dot{\theta}$	Leg compression and swing rates
m, g	Body mass and gravitational acceleration
c, k	Leg damping constant and stiffness
r_0	Leg rest length
$r_{\text{td}}, \theta_{td}$	Touchdown leg length and angle
$z_a, \dot{y}_a$	Apex height and horizontal velocity

However, system dynamics during stance is not as simple as in the flight phase. In order to obtain the equations of motion during the stance phase, Lagrangian method is used in this paper. In the non-dimensional formulation, Lagrangian of the system dynamics can be obtained as

$$L = \frac{1}{2}(\dot{r}^2 + r^2\dot{\theta}^2) - \frac{k}{2}(1-r)^2 - r\cos\theta. \tag{2}$$

In addition, we have a Rayleigh dissipation function due to the damping term as

$$D = \frac{1}{2}c\dot{r}^2. \tag{3}$$

By using the classical Lagrange's equations

$$\frac{\mathrm{d}}{\mathrm{d}t}\left(\frac{\partial L}{\partial \dot{q}_j}\right) - \frac{\partial L}{\partial q_j} + \frac{\partial D}{\partial \dot{q}_j} = 0, \tag{4}$$

with $q_1 = r$ and $q_2 = \theta$, we obtain the following equations of motion for the stance phase

$$\ddot{r} = r\dot{\theta}^2 + k\,(1-r) - \cos\theta - c\dot{r}, \tag{5}$$

$$\ddot{\theta} = \frac{1}{r}\left(\sin\theta - 2\dot{r}\dot{\theta}\right). \tag{6}$$

It has been shown that the equations of the form given by (5) and (6) are non-integrable [24]. Hence, exact analytical solution of the stance dynamics given by (5) and (6) is not available. Although numeric integration is a first choice to obtain stance trajectories, it is not an efficient solution for online computation when solutions with different parameter sets are needed to optimize the controller parameters [26]. Some researchers proposed analytical approximate solutions to the stance dynamics [9,27], some with iterative solutions [23] and some of these approximations are validated on physical robot platforms [28]. On the other hand, some studies in the literature focus on using partial feedback linearization, which aims at deriving exact analytical solutions with the utilization of additional actuators [29].

2.2 Active SLIP model

In this section, we give a brief review of the active SLIP model proposed in [29]. Note that [29] utilizes partial feedback linearization to obtain exact analytical solutions to originally non-integrable system dynamics. More precisely, a linear actuator is attached to the leg spring serially and the length of the actuator can be adjusted. By adjusting actuator length, some nonlinear elements are canceled and the resulting system dynamics may have analytical solutions.

The addition of linear actuator changes the leg length as

$$r(t) = r_{\text{act}}(t) + r_k(t) \tag{7}$$

where $r_{\text{act}}(t)$ represents the linear actuator length and $r_k(t)$ is leg spring length. In the same formulation, the symbols $r_{\text{act},0}$ and $r_{k,0}$ are used to describe the rest

lengths of the linear actuator and the leg spring, respectively. Therefore, the leg rest length can be represented as $r_0 = r_{k,0} + r_{\text{act},0}$.

Actuator displacement is defined as $\Delta r_{act} = r_{\text{act}} - r_{\text{act},0}$ in [29]. For Δr_{act}, the following control law is proposed in [29]

$$\Delta r_{act} = \frac{m}{k}\left(\ddot{r} + g\cos\theta - r\dot{\theta}^2\right) + r - r_0, \tag{8}$$

for the actuator displacement to make the point mass to follow the desired trajectory.

In order to obtain analytically tractable equations of motion for the stance phase, [29] forces the point mass to follow some specified symmetric gaits. For instance, the following equation for the angular velocity is used to enforce the symmetric gait in [29]

$$\dot{\theta}(t) = A\cos\theta(t) + c_1, \tag{9}$$

where A and c_1 are determined from the boundary conditions between descent and compression sub-phases at the touchdown instant. The solutions of $A, c_1, r(t)$ and more details can be found in [29].

One important note is that the quantities given in this section is not in non-dimensional formulation in order to book-keep the notation of [29].

2.3 Torque-actuated dissipative SLIP model

In this section, we review the torque-actuated dissipative SLIP (TD-SLIP) model, proposed by Ankarali and Saranli [20]. One of the main contributions of this model is that a rotary actuator is attached to the hip to compensate the damping loss of the dissipative SLIP model. The aim of this work is to approximate stance dynamics of the proposed model and to perform limit cycle identification and characterization.

It has been shown in [20] that TD-SLIP model is marginally stable without applying an explicit control but asymptotically stable locomotion can be achieved for fixed touchdown angles by applying torque inputs via the hip actuator.

For the hip actuator, the following torque function is proposed in [20]

$$\tau(t) = \begin{cases} \tau_0(1 - t/t_f) & \text{if } 0 \le t \le t_f \\ 0 & \text{if } t > t_f \end{cases} \tag{10}$$

where $\tau_0 := \alpha/\dot{\theta}_{td}$. The α parameter is called as constant touchdown parameter. This function is simple and uses some constants that is determined before touchdown event. Also, the decreasing nature of this function avoids the application of negative work during stance. In order to ensure that torque applied at the liftoff instant is zero, t_f is chosen as the liftoff time. By this way, the hip torque does not cause early liftoffs and the stance duration approximation does not become difficult. More details about this model and derivations can be found in [20].

3 Multi-actuated dissipative SLIP model

3.1 Model and dynamics

The proposed model differs from the original SLIP template by the addition of two actuators as stated earlier. These actuators help us to use partial feedback linearization methods to obtain analytic solutions to the stance dynamics. The first actuator is a linear motor that is attached serially to the leg spring. The second actuator on the other hand is a rotary actuator that is attached to the point mass at the hip to apply the rotational torque τ. This model is called as multi-actuated dissipative SLIP template and is shown in Fig. 4, where the coordinate system, model parameters and the additional actuators are also illustrated. Note that although the SLIP template (and hence our proposed model) can be used to represent center of mass trajectories of different animals with varying number of legs (see Sect. 1.1), the SLIP model itself (and hence our proposed model) corresponds to a one-legged hopping robot when simulated in computerized environments.

Note that our additional actuators do not violate or change the assumptions on the original SLIP model such as point mass and massless leg. Therefore, point mass still follows a ballistic trajectory during the flight phase, so the equations of motion will be same as in (1). However, addition of two new actuators changes the stance dynamics, since now we are capable of injecting and removing energy from the system. Therefore, the modified stance dynamics for the multi-actuated dissipative SLIP (MD-SLIP) model can be given as

$$\ddot{r} = r\dot{\theta}^2 + k\,(1 - r + \Delta r_{act}) - \cos\theta - c\dot{r}, \tag{11}$$

$$\ddot{\theta} = \frac{1}{r}\left(\sin\theta - 2\dot{r}\dot{\theta}\right) + \frac{\tau}{r^2}, \tag{12}$$

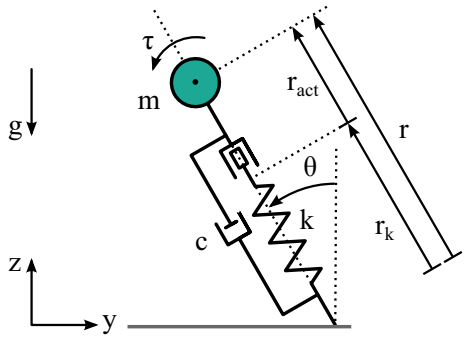

Fig. 4 Multi-actuated dissipative SLIP model, coordinate system and model parameters. The difference of this model with the dissipative SLIP model (illustrated in Fig. 1) is the addition of the linear and the rotary actuators

where $\Delta r_{act} = r_{\text{act}} - r_{\text{act},0}$.

We note that all time-dependent functions in Sect. 3 use touchdown time as reference for the sake of simplicity.

3.2 Solving stance dynamics

As mentioned before, the stance dynamics of the SLIP model does not have exact analytical solution due to its highly nonlinear and non-integrable nature. This problem may become more complex if Δr_{act} and τ in (11)–(12) are not chosen appropriately. In this part, we explain how we can obtain exact analytical solutions to the stance dynamics of the MD-SLIP model by canceling some nonlinear terms in the system dynamics. We show that Eqs. (11) and (12) can be solved when partial feedback linearization is used to cancel out some nonlinear terms. Besides, partial feedback linearization can also be used to enforce specific solutions to Eqs. (11) and (12) such as specifying some desired trajectories to the point mass during its stance locomotion.

To cancel some of the nonlinear terms in Eq. (11), linear actuator displacement is chosen as

$$\Delta r_{act} = \frac{1}{k}(\cos\theta - r\dot{\theta}^2 + c\dot{r}) - A_0 + C_0 t, \tag{13}$$

where A_0 can be used to adjust the initial value and C_0 can be used as an additional control parameter.

At touchdown instant, a force is applied to the point mass in order to compensate the losses due to leg damping. To achieve this, Δr_{act} is chosen as $c\dot{r}_{td}/k$ at touchdown instant. Using this idea and evaluating (13) at touchdown instant, we obtain:

$$A_0 = \frac{\cos\theta_{td} - r_{\text{td}}\dot{\theta}_{td}^2}{k}. \tag{14}$$

Substituting (13) in (11) results in

$$\ddot{r} + kr = k(1 - A_0 + C_0 t). \tag{15}$$

The solution of (15) can be obtained as

$$r(t) = A_1 \sin(\omega t) + A_2 \cos(\omega t) + 1 - A_0 + C_0 t \tag{16}$$

where $w = \sqrt{k}$.

Applying the boundary condition at touchdown instance, i.e., the leg length should be equal to the leg rest length, A_2 can be found as $A_2 = A_0$.

In order to find the A_1, the radial velocity

$$\dot{r}(t) = A_1\omega\cos(\omega t) - A_0\omega\sin(\omega t) + C_0, \tag{17}$$

should be equal to its touchdown value at touchdown instant, which results in

$$A_1 = \frac{\dot{r}_{td} - C_0}{\omega}. \tag{18}$$

As a result, the leg length during stance phase can be found as

$$r(t) = 1 - A_0 + A_0\cos(\omega t) + A_1\sin(\omega t) + C_0 t, \tag{19}$$

where A_0 and A_1 are given by (14) and (18), respectively.

For the angular velocity equation (12), we propose an approach similar to the one utilized in [29]. By adding an additional control parameter C_1, similar to (9), we propose the following desired angular velocity equation

$$\dot{\theta} = B_0\cos(\theta + C_1) + B_1. \tag{20}$$

The required torque to enforce (20) can be found from (12) as

$$\tau = 2r\dot{r}\dot{\theta} - r\sin\theta - B_0 r^2\sin(\theta + C_1)\dot{\theta}. \tag{21}$$

In order to avoid sudden jumps in torque, we chose to apply $\tau = 0$ at touchdown instance. Using this decision in (21), we obtain

$$B_0 = \frac{2\dot{r}_{td}\dot{\theta}_{td} - \sin\theta_{td}}{\sin(\theta_{td} + C_1)\dot{\theta}_{td}}. \tag{22}$$

Furthermore, by evaluating (20) at touchdown instance we obtain

$$B_1 = \dot{\theta}_{td} - B_0 \cos(\theta_{td} + C_1). \tag{23}$$

Solving the angular velocity equation (20) for the angular position results in

$$\theta(t) = \frac{\pi}{2} - C_1 + 2\text{atan}\left(\frac{B_0 - B_2 \tanh\left(\frac{B_2 t}{2} + B_3\right)}{B_1}\right), \tag{24}$$

where B_2 and B_3 are defined as

$$B_2 := \sqrt{B_0^2 - B_1^2}, \tag{25}$$

$$B_3 := \text{atanh}\left(\frac{B_0 + B_1 \tan\left(\frac{\theta_{td} + C_1 - \frac{\pi}{2}}{2}\right)}{B_2}\right). \tag{26}$$

After some lengthy but straightforward calculations, we obtain the following equation for the angular position

$$\theta(t) = \theta_{td} + 2\text{acot}\left(\frac{B_2\dot{\theta}_{td}\coth\left(\frac{B_2 t}{2}\right) + 2\dot{r}_{td}\dot{\theta}_{td} - \sin\theta_{td}}{\dot{\theta}_{td}^2}\right). \tag{27}$$

To summarize, if we choose the linear actuator control law as in (13), the solution of the radial dynamics given by (11) can be obtained as (19), where A_0 and A_1 are constants that are obtained as (14) and (18), respectively, and C_0 is a free control parameter. Likewise, if we use the torque control law as in (21), the solution of the angular dynamics given by (12) can be obtained as (27), where B_0, B_1 and B_2 are constants as given by (22), (23) and (25), respectively, and C_1 is a free control parameter.

Note that stance trajectories generated by (19) and (27) are not arbitrary functions enforced by partial feedback linearization. Actually, these trajectories are well-fitted locomotion trajectories similar to the ones generated by the SLIP model. A sample stance trajectory is shown in Fig. 14.

Remark 1 We note that both the solutions given by (19) and (27) depend on the touchdown positions and velocities. Since the flight phase dynamics are integrable, these values can be obtained at the end of the flight phase, then (19) and (27) could be used as the solutions of stance phase dynamics. Moreover, these formulas contain the free control parameters C_0 and C_1 explicitly; hence, by choosing these parameters appropriately, one may achieve various control objectives.

3.3 Apex-to-apex return map

In order to understand and analyze the MD-SLIP model in detail, its locomotion needs to be divided into sub-phases that consecutively repeat themselves. In this paper, we choose the starting phase as the apex instance and use the apex-to-apex return map to represent the locomotion. The states at the current apex point are chosen as the apex height z_{a0} and apex velocity $\dot{y}_{a0}$. When the locomotion starts from the apex state, it follows the ballistic trajectory (1) until the toe touches to the ground. It means, the touchdown event occurs when the equation $z = \cos\theta_{td}$ is satisfied. Hence, the state variables of the descent sub-phase and their relations can be written as

$$(\dot{z}_{\text{td}}, \dot{y}_{\text{td}}) = F_a^{\text{td}}(z_{a0}, \dot{y}_{a0}), \tag{28}$$

where the subscript td indicates the touchdown, F_a^{td} is the apex to touchdown map, the velocities $\dot{z}_{\text{td}}$ and $\dot{y}_{\text{td}}$ are vertical and horizontal velocities in Cartesian coordinates at touchdown instance, respectively. Note that the map F_a^{td} depends on θ_{td} which is considered as a control parameter. The latter approach is utilized in various control schemes proposed for SLIP dynamics; see, e.g., [1,25,26].

After the toe touches the ground, the point mass starts to follow the stance dynamics (11) and (12) which are solved as (19) and (27). The function for the stance phase can be written as

$$(r_{\text{lo}}, \dot{r}_{\text{lo}}, \theta_{\text{lo}}, \dot{\theta}_{\text{lo}}) = F_{\text{td}}^{\text{lo}}(\dot{r}_{\text{td}}, \dot{\theta}_{\text{td}}), \tag{29}$$

where the subscript lo indicates the liftoff and $F_{\text{td}}^{\text{lo}}$ is the touchdown to liftoff map. Note that the map $F_{\text{td}}^{\text{lo}}$ depends on the control parameters θ_{td}, C_0 and C_1, see (19) and (27).

The liftoff event occurs, when the toe loses ground contact. After this instance the point mass follows the ballistic trajectory (1) again until its vertical velocity becomes zero at the apex. The ascent sub-phase can be represented as

$$(z_{a1}, \dot{y}_{a1}) = F^a_{\text{lo}}(\dot{z}_{\text{td}}, \dot{y}_{\text{td}}, r_{\text{lo}}, \theta_{\text{lo}}), \tag{30}$$

where F^a_{lo} is the liftoff to apex map.

After describing the trajectory from current apex state to the next one, apex-to-apex function can be written as

$$F^a_a = F^a_{\text{lo}} \circ R_{\text{lo}} \circ F^{\text{lo}}_{\text{td}} \circ R_{\text{td}} \circ F^{\text{td}}_a, \tag{31}$$

where F^a_a represents apex-to-apex return map. Note that R_{td} and R_{lo} stands for the coordinate transformations between Cartesian and polar coordinates. These transformations are required since we use polar coordinates for our stance phase (radial) solutions while the actual map (with descent and ascent phases) are represented in Cartesian coordinates.

Finally, the next apex state can be achieved by using current apex state as

$$(z_{a1}, \dot{y}_{a1}) = F^a_a(z_{a0}, \dot{y}_{a0}), \tag{32}$$

where z_{a1} and $\dot{y}_{a1}$ are the height and the velocity at the next apex point. Note that the map F^a_a depends on the control parameters θ_{td}, C_0 and C_1. Our aim is now to choose these control parameters appropriately to obtain stable gait patterns.

Remark 2 The apex-to-apex return map, F^a_a, is important in studying the possible running gait patterns of the SLIP dynamics as well as stability of such gaits. For example, any periodic gait is a fixed point of F^a_a, and any stable gait is a stable fixed point of F^a_a.

3.4 Finding stance duration

To find the stance duration, the liftoff condition needs to be determined. In the dissipative SLIP model, leg spring is constrained such that the maximum length of the leg spring is its rest length. On the other hand, dissipation in the SLIP model can yield some early liftoffs. In addition to these two criteria, we avoid negative work by turning off the torque control to ensure early liftoff. Hence, the liftoff condition can be given as

$$r = 1 + \Delta r_{act} - \frac{c}{k}\dot{r}, \tag{33}$$

where Δr_{act} is given by (13). Due to the highly nonlinear expressions of the latter, finding an analytical expression for the solution of (33) is very difficult. However, the numeric calculation is still a way to find the stance duration.

Under the symmetric stance trajectory assumption, we can find exact solution for the stance duration. To have symmetric stance trajectory, leg length and leg angle need to be even and odd symmetric around the time halfway through the stance phase, respectively [1]. To satisfy these requirements, three conditions need to be met. First, leg length needs to be even symmetric around bottom event, which is possible by choosing $C_0 = 0$. Second, leg angle needs to be odd symmetric, which requires $C_1 = 0$. Third, at bottom time leg angle should be zero. As a result, a symmetric gait is formed by choosing control parameters C_0 and C_1 as zero and adjusting θ_{td} to tune the bottom time

$$t_b = \frac{1}{w}\left(\pi - \text{acos}\left(\frac{A_0}{\sqrt{A_0^2 + A_1^2}}\right)\right) \tag{34}$$

and the time required to make θ zero

$$t_{\theta 0} = \frac{2}{B_2}\text{acoth}\left(\frac{\sin\theta_{td} - \dot{\theta}^2_{td}\cot(\frac{\theta_{td}}{2}) - 2\dot{r}_{td}\dot{\theta}_{td}}{B_2\dot{\theta}_{td}}\right) \tag{35}$$

equal. Then, the stance duration can be calculated as

$$t_s = 2t_b = 2t_{\theta 0}. \tag{36}$$

4 Periodic gaits and their stability in MD-SLIP model

As stated in Remark 2, the periodic gaits of the proposed MD-SLIP model are the fixed points of the apex-to-apex map F^a_a given by (31). This fixed point, $(z^*_a, \dot{y}^*_a)$, satisfies the following equation

$$(z^*_a, \dot{y}^*_a) = F^a_a(z^*_a, \dot{y}^*_a). \tag{37}$$

The stability of such fixed points can be determined by the eigenvalues of the Jacobian matrix of F_a^a evaluated at the fixed point. The Jacobian matrix is defined for the apex-to-apex return map as

$$J := \begin{bmatrix} \frac{\partial z_{a1}}{\partial z_{a0}} & \frac{\partial z_{a1}}{\partial \dot{y}_{a0}} \\ \frac{\partial \dot{y}_{a1}}{\partial z_{a0}} & \frac{\partial \dot{y}_{a1}}{\partial \dot{y}_{a0}} \end{bmatrix}. \tag{38}$$

However, we do not have exact solution of the stance duration for all cases, where numeric calculation might be necessary. In such cases, the Jacobian matrix is approximated in numerical simulations as

$$J_n := \begin{bmatrix} \frac{z_{a1z} - z_{a1}}{\Delta z_{a0}} & \frac{z_{a1y} - z_{a1}}{\Delta \dot{y}_{a0}} \\ \frac{\dot{y}_{a1z} - \dot{y}_{a1}}{\Delta z_{a0}} & \frac{\dot{y}_{a1y} - \dot{y}_{a1}}{\Delta \dot{y}_{a0}} \end{bmatrix}, \tag{39}$$

where the values for Δz_{a0} and $\Delta \dot{y}_{a0}$ have been chosen as sufficiently small values to approximate the numerical derivatives. After some extensive simulations, we experimentally choose this number as 10^{-5}, since further decrease apparently does not have a meaningful change on the eigenvalues of the Jacobian. The other variables are defined as

$$(z_{a1}, \dot{y}_{a1}) := F_a^a(z_{a0}, \dot{y}_{a0}), \tag{40}$$

$$(z_{a1z}, \dot{y}_{a1z}) := F_a^a(z_{a0} + \Delta z_{a0}, \dot{y}_{a0}), \tag{41}$$

$$(z_{a1y}, \dot{y}_{a1y}) := F_a^a(z_{a0}, \dot{y}_{a0} + \Delta \dot{y}_{a0}). \tag{42}$$

During simulations, the non-dimensional parameters and initial conditions are chosen as $z_a \in [1 - 2]$, $\dot{y}_a \in [0 - 3.2]$ and $k \in [15 - 100]$.

4.1 Zero control parameters C_0 and C_1

The goal of this section is to investigate the stability of the periodic motion for the proposed MD-SLIP model when the gaits are symmetric.

Note that symmetric gaits are obtained by choosing the control parameters C_0 and C_1 as zero leaving us the leg touchdown angle, θ_{td}, as the only control parameter to regulate the gait. In order to begin stability analysis, fixed points of the corresponding Poincaré map should be extracted. To accomplish this, we first find the touchdown angle, θ_{td} that yields same solutions for (34) and (35) to obtain the fixed point manifold. At this point, we use numeric calculations to solve $t_b = t_{\theta 0}$ in order to find the fixed point manifold since obtaining an analytic solution is very difficult for these equations; see (34) and (35). The significance of this fixed point manifold is that any point chosen inside the fixed point manifold as an initial condition to our MD-SLIP model yields periodic locomotion. The fixed point manifold of the MD-SLIP model in terms of a function apex height, apex velocity and touchdown angle is illustrated in Fig. 5.

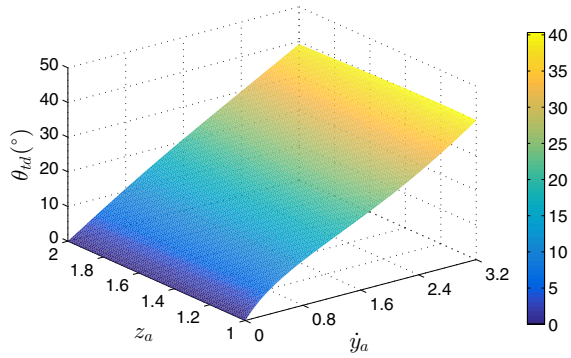

Fig. 5 Touchdown angles that result periodic gaits for the MD-SLIP model with control parameters C_0 and C_1 are zero. The dimensionless spring constant k is chosen as 36

Another important observation about Fig. 5 is that the touchdown angle θ_{td} that results in periodic motion is more or less proportional to the apex horizontal velocity $\dot{y}_a$. Note that this property is also observed in the original SLIP template and [1] designed touchdown angle controllers to regulate apex horizontal velocity based on this principle. Figure 5 shows that our proposed model also exhibits this property, which would allow simple touchdown angle controllers as in [1] to regulate apex horizontal velocity. We note that average steady-state velocity is utilized as a measure to determine the locomotion performance in [5]. By combining this idea with the observation given above, we could state that if we choose apex horizontal velocity as a measure to evaluate the locomotion performance, we could utilize the touchdown angle as a parameter for optimizations. However, since our main aim in this work is to determine the existence and stability of periodic gaits, we do not elaborate further on this subject which requires and deserves further investigation.

Having zero control parameters assumption, we have analytic solutions to the system dynamics and stance duration, and hence, we can perform an analytic stability analysis. However, the stance duration is solved only for the symmetric gaits and this analysis requires the general solution for the stance duration.

Since the analysis is performed around the symmetric stance trajectories, we assume that the stance duration equation solved for symmetric gaits can be used in this analysis. Additionally, finding an exact analytic solution for the leg touchdown angle that results in periodic locomotion is very challenging. Therefore, we utilize numeric solution to find leg touchdown angles and plug in these numeric solution into our equations to form the Jacobian matrix. Symbolic Toolbox of the MATLAB is used in all the steps to calculate the eigenvalues for the Jacobian matrix (38), because of the complexity of the equations. Since we perform the analysis around the symmetric gaits, magnitude of one of the eigenvalues always results as 1. Therefore, we use the magnitude of the other eigenvalue to determine the stability of the gaits.

Note that using analytical Jacobian for computing eigenvalues is only valid for symmetric gaits. However, most of the natural gaits generated by animals, and hence our simulation models, correspond to asymmetric trajectories, which requires derivation of numeric Jacobian matrix as in (39). In order to validate this approach, we first derived both analytical and numerical Jacobian matrices for the symmetric gait assumption and compared the resulting eigenvalues. Having noticed that the distance between first eigenvalue pair was less than 0.1% (the other eigenvalue pair was equal to 1 in both approaches), we decided to proceed with (39) to compute eigenvalues for the non-symmetric gaits.

To compare the stability of the periodic gaits for the MD-SLIP model and the SLIP model, fixed points of the corresponding apex-to-apex map should be obtained. To find the fixed points of the periodic gaits for the SLIP model, conservation of energy is required. Therefore, we choose the damping constant as zero to find the fixed points of the SLIP model and perform a stability analysis to compare with the MD-SLIP model. In Fig. 6, stability regions of SLIP model and MD-SLIP model is shown. It is obvious that MD-SLIP model increases the stable region for the interested region of initial conditions.

Remark 3 Note that our stability analysis is based on the linearization of nonlinear dynamics around a periodic motion (i.e., limit cycle). As a result of linearization, all of our results are only local; hence, stable periodic gait here means an asymptotically (and locally) stable periodic motion; see [38]. There are various ways

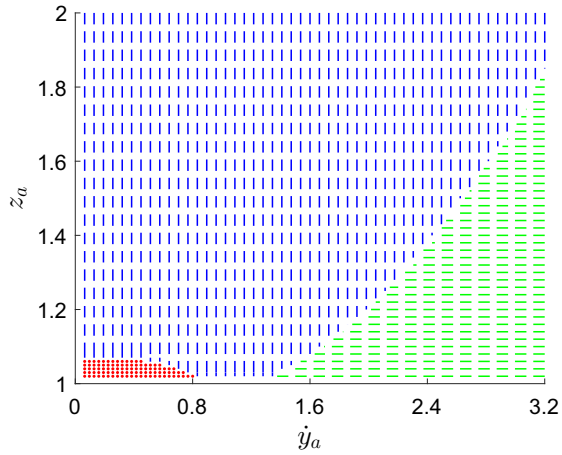

Fig. 6 A Comparison between stability regions of the SLIP and MD-SLIP models. *Blue* (*vertically dashed*) region illustrates the stable gaits of the MD-SLIP model and *green* (*horizontally dashed*) region illustrates the stable region for both SLIP and MD-SLIP models. Finally, the *red* (*dotted*) region illustrates the region where both models are unstable. Note that the dimensionless spring constant is chosen as 36 in this analysis. (Color figure online)

to measure the stability performance of the periodic gaits considered in this work. An obvious choice would be to characterize or estimate the domain of attraction (DoA) of such a gait (i.e., the set of all initial apex states from which the starting trajectories asymptotically converge to the apex state of the periodic gait). However, finding and/or estimating such a DoA is quite difficult and requires mainly large amount of simulations; see, e.g., [38,39], which is beyond the scope of present work. Another measure is the robustness of such stable gaits against small perturbations, and rough terrain simulations are frequently utilized in the literature as a measure of such robustness, [15,22,39]. Indeed, our stable gaits are found when SLIP motion is on a flat ground. When the terrain changes, its effect could be considered as a perturbation of apex state and if the resulting motion still converges to the periodic gait in question in rough terrains, this would indicate a sufficiently robust stable gait. Although an exact analytical relation between this type of robustness measure and the size of DoA is not available, we may expect that the better robustness results in rough terrain simulations is an indicator of larger sizes for DoA. This approach will be utilized in Sect. 5; see also [39] for similar stability measures. Another measure for stability performance might be the magnitude of the maximum eigenvalue;

see, e.g., [39]. Minimization of this quantity as a stability measure will be considered in Sect. 4.2. We note that other measures of stability, as well as estimation of DoA, are subjects which require and deserve further investigations.

Since active SLIP model proposed in [29] enforces a symmetric gait for all initial conditions, the Jacobian matrix becomes identity matrix. Hence, the eigenvalues of the Jacobian matrix becomes 1. Therefore, our approach which is based on linearization is inconclusive to determine the stability properties of periodic gaits obtained in [29]. As a result, we cannot compare the stability of the periodic gaits for the MD-SLIP model and the model given in [29] by using our method.

On the other hand, we could compare the properties of stable gaits obtained in our model with the ones obtained in TD-SLIP model. The fixed points of the TD-SLIP are calculated and the stability analysis for TD-SLIP is also performed. In order to make a fair comparison, non-dimensional spring constant k is chosen as 36 and non-dimensional damping coefficient c is chosen as 0.96 to satisfy the value 0.08 for the damping ratio ζ_0 as in [20]. The stability regions of the periodic gaits of TD-SLIP model and MD-SLIP model are illustrated in Fig. 7. When we compare the stability regions of the gaits generated by the proposed model with the TD-SLIP model, we notice that the MD-SLIP model increases the region in which stable motion is observed. There is only a very small portion in our initial condition range, where the TD-SLIP model generates stable gaits but the proposed model gaits are unstable; note that this region is very small and corresponds to initial conditions with heights very close to leg length and very small horizontal velocities. On the other hand, the proposed model exhibits stable gaits in a wide range of initial conditions, where TD-SLIP model is unable to preserve the stability of gaits.

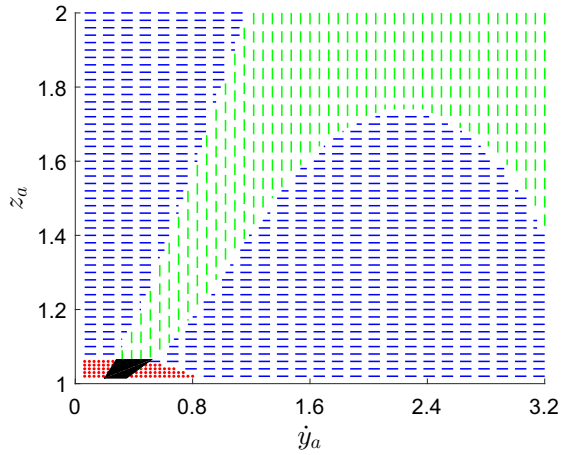

Fig. 7 Stability regions for the TD-SLIP and MD-SLIP models. *Green* (*vertically dashed*) and *red* (*dotted*) regions illustrate the stability and instability for both models, respectively. *Blue* (*horizontally dashed*) region corresponds to stability region for MD-SLIP model, while TD-SLIP is unstable. On the contrary, *black* (*shaded*) region represents stability region for the TD-SLIP model while the MD-SLIP model is unstable. The dimensionless spring and damping constants k and c are chosen as 36 and 0.96, respectively. (Color figure online)

4.2 Optimizing control parameters C_0 and C_1

In this section, we investigate the stability of periodic gaits when $C_0 \neq 0$ and/or $C_1 \neq 0$ case. As we mentioned before, the case $C_0 = C_1 = 0$ results is symmetric gaits, and when $C_0 \neq 0$ and/or $C_1 \neq 0$, the resulting gait becomes asymmetric. We also observed that in this case, the resulting periodic motion has better stability characteristics as compared to symmetric periodic gait case. Hence, by choosing C_0 and C_1 appropriately we may improve some stability measures. As noted in Remark 3, maximum eigenvalue magnitude will be used as a stability measure in this section. More precisely, let λ_1 and λ_2 be the eigenvalues of the Jacobian matrix. Then the optimization problem considered in this section is given as

$$\min_{\theta_{\text{td}}, C_0, C_1} \max\{|\lambda_1|, |\lambda_2|\}. \tag{43}$$

For a given $w^* = (z_a^*, \dot{y}_a^*)$ pair, if we choose $C_0 = C_1 = 0$, then there is a single touchdown angle θ_{td} value which makes w^* a fixed point. However, if we choose $C_0 \neq 0$ and/or $C_1 \neq 0$, then there is a range of touchdown angle θ_{td} values which make w^* a fixed point for a given $w^* = (z_a^*, \dot{y}_a^*)$ pair. The magnitudes of the eigenvalues of the corresponding Jacobian matrix for the changing touchdown angle θ_{td} are illustrated in Fig. 8. Minimizing the touchdown angle while keeping the eigenvalues in the unit circle results in $C_0 = C_1 = 0$. Maximum values for the touchdown angle while keeping the eigenvalues in the unit circle is illustrated in Fig. 9. It is seen that the range for stable touchdown angle can go up to 10 degrees by comparing Fig. 5 and 9. Notice that proportionality between the touchdown angle θ_{td} that results in periodic motion and

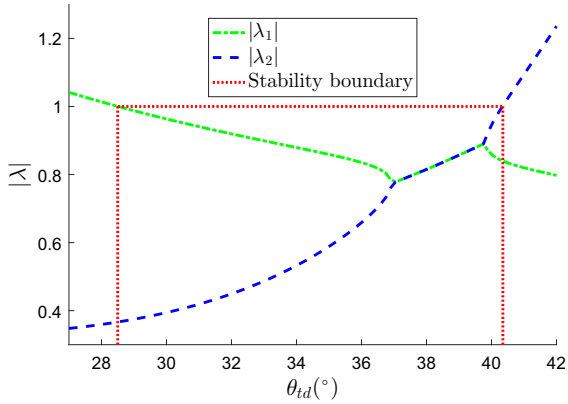

Fig. 8 Magnitudes of the eigenvalues with respect to touchdown angle. The *green* and *blue lines* correspond to two eigenvalues of the system with respect to varying touchdown angles. The *red* (*dotted*) lines represent the stability boundary. In this system, the touchdown angle is chosen appropriately by adjusting C_0 and C_1 to make the gaits fixed point. The dimensionless apex height and velocity are 1.02 and 2.3, respectively. (Color figure online)

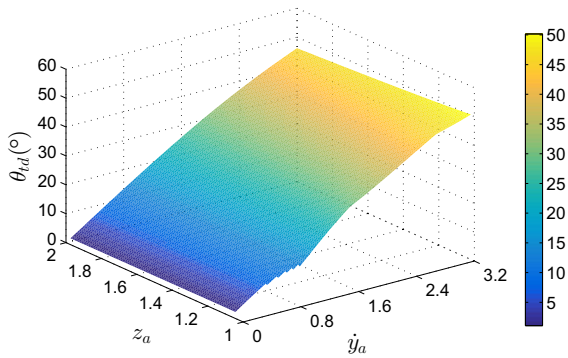

Fig. 9 Touchdown angles that result periodic gaits for the MD-SLIP model with control parameters C_0 and C_1 are optimized to maximize the touchdown angle while keeping magnitudes of the eigenvalues of the Jacobian matrix of the apex-to-apex map in the unit circle. The dimensionless spring constant k is chosen as 36. Terrain 1 is the simple flat ground which is used in comparison with the terrains 2–7

the apex horizontal velocity $\dot{y}_a$ is still valid for asymmetric gaits. Therefore, simple touchdown angle controllers as in [1] can also be used for asymmetric gaits in the proposed model. As noted in Sect. 4.1, following the idea given in [5], if we choose apex horizontal velocity as a measure for locomotion performance, we could utilize touchdown angle as a control parameter for optimization.

To provide some insight about the asymmetry of the gait, the angle bisector of the touchdown angle θ_{td} and liftoff angle θ_{lo} is chosen as a measure. Notice

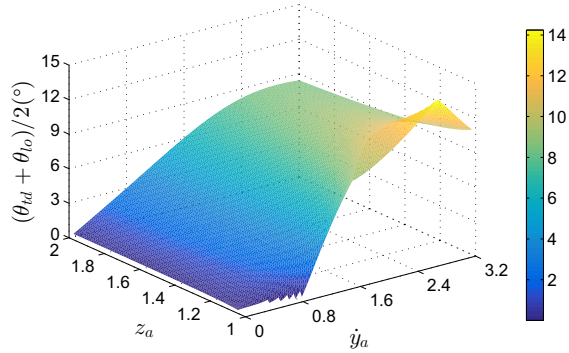

Fig. 10 Angle bisector of touchdown and liftoff angles of the MD-SLIP model. The control parameters, C_0 and C_1, are adjusted to obtain a stable system (eigenvalues are inside the *unit circle*) with maximum touchdown angle to compute the angle bisector. The dimensionless spring constant is chosen as 36 in this test

that increased angle bisector results in increased asymmetry. For stable gaits, it is observed that maximum values for the angle bisector is observed around maximum touchdown angles. Angle bisector for maximum touchdown angle case is shown in Fig. 10.

5 Performance of MD-SLIP model on rough terrain

5.1 Open-loop control with fixed control parameters

As stated in Remark 3, one way of evaluating the stability of periodic gaits is to utilize rough terrain simulations, which gives us a measure of robustness of the corresponding periodic motion. In this section, we present various rough terrain simulations to test the robustness of the periodic gaits of three models introduced before, namely SLIP, TD-SLIP and MD-SLIP models. We utilize successful running (i.e., running without falling) rates as a robustness measure and show that the results obtained in Sect. 4 actually yield sufficiently robust, hence stable, periodic gaits.

Section 4 investigates the stability performance of the gaits for the three models, SLIP, TD-SLIP and MD-SLIP, by checking the eigenvalues of the Jacobian matrix around a periodic trajectory. This corresponds to linearizing the dynamics around a periodic function. In order to have an insight about the region of attraction (validity region for our stability analysis), this section presents the results for stability performance of the

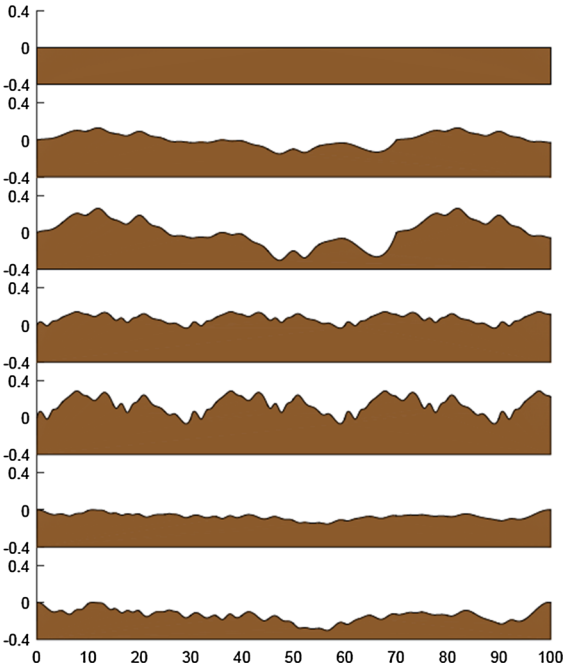

Fig. 11 Terrains 1–7 used during the simulations. Terrain 1 is the simple flat ground which is used in comparison with the terrains 2–7

Table 3 Properties of the Terrains

Terrain	Mean	Variance	Average Power
1	0.00000	0.00000	0.00000
2	−0.01719	0.00552	0.00581
3	−0.03438	0.02207	0.02322
4	0.06568	0.00228	0.00659
5	0.13136	0.00911	0.02636
6	−0.07099	0.00112	0.00616
7	−0.14199	0.00449	0.02465

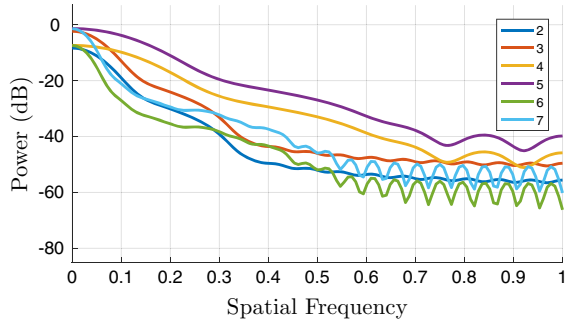

Fig. 12 Power spectral density for the terrains 2–7

three models on rough terrain running experiments. We show that the results obtained in Sect. 4 do not simply yield a local stability but they correspond to gaits that are robust to different rough terrains.

The proposed model, MD-SLIP model, is compared with the TD-SLIP model and the original SLIP model on different terrains, which are depicted in Fig. 11. Mean, variance and average power of the terrains are given in Table 3. Average powers of the terrains are obtained via simple computations (square of the terrain signal integrated over a period normalized by the length of the period) due to the periodicity of the terrains. Additionally, power spectral density of the terrains is illustrated in Fig. 12 that are computed by the Welch's method [40]. Hence, the intuitive difference between the terrains depicted in Fig. 11 can be quantitatively observed from Table 3 and Fig. 12.

In order to generalize our results, we performed our tests with various initial conditions, where the dimensionless spring and damping constant were chosen as $k = 36$ and $c = 0.96$, respectively, in order to reach optimum performance of the TD-SLIP model for a fair comparison. For the initial conditions, we chose 100 linearly spaced values for $z_a \in [1.01 - 2]$ and 100 linearly spaced values for $\dot{y}_a \in [0.032 - 3.2]$ that yields a total number of 10,000 initial condition points.

In order to perform our analysis in steady state, we first simulate the models for 1000 steps on the seven terrain models that are depicted in Fig. 11 and count the successful runs. The step number, 1000, is chosen experimentally to make sure that further increasing the step number does not affect our performance criteria. We note that we also performed the same simulations for 100 steps. Although the success/failure rates given in Tables 4, 5 and 6 change slightly, the general tendency which indicates that MD-SLIP model outperforms the other SLIP templates remained the same. Further increasing the step size apparently does not change this conclusion. Following these observations, we fixed the step size to 1000 for this section. Also as noted in Remark 3, rough terrain simulations are expected to give an indication on the robustness of stability of periodic gaits; hence, from this perspective, we could consider the success/failure rates given in Tables 4, 5 and 6 as a measure for stability performance. Table 4 lists the percentage failures for the three models on different terrains (Here, a successful run corresponds to a case where the SLIP model completes 1000 steps without

Table 4 Percentage of the data points that failed to achieve 1000 steps on the given terrains

Terrain	Model		
	SLIP	TD-SLIP	MD-SLIP
1	77.67	35.29	**2.74**
2	83.35	64.40	**21.20**
3	90.58	71.20	**37.50**
4	90.99	56.67	**20.50**
5	95.81	68.37	**36.21**
6	65.44	40.15	**10.95**
7	77.24	48.19	**20.03**

Table 5 Percentage of the data points that cannot stand for additional 1000 steps on the flat ground in addition to the 1000 steps in the given terrains

Terrain	Model		
	SLIP	TD-SLIP	MD-SLIP
1	78.38	35.37	**2.79**
2	85.96	64.54	**21.26**
3	91.70	71.28	**37.58**
4	90.99	56.67	**20.50**
5	95.81	68.41	**36.21**
6	70.78	41.76	**15.84**
7	82.69	50.11	**26.00**

falling). As can be seen, MD-SLIP model outperforms the other models with a mean failure error of 21.30% on seven terrains.

Having identified the successful runs on rough terrain, we continue to simulate the models for another 1000 steps on flat ground to investigate the robustness of the resulting periodic gaits. Our aim in these simulations is to observe whether the runs which successfully finish 1000 steps in a rough terrain (without falling) would continue to run successfully on a flat ground for another 1000 steps; hence, the resulting periodic gait is robust in this sense. Table 5 lists the percentage of failure for the three models which could not stand for another 1000 steps on. As can be seen, the MD-SLIP model outperforms the other models in this test.

The final step in our performance observation is to determine whether the initial and final apex states in our simulations for the three models in flat ground following these rough terrains are sufficiently close. If $w_i = (z_a^*, \dot{y}_a^*)$ is the initial apex state and $w_f = (z_{\text{af}}, \dot{y}_{\text{af}})$ is the final apex state (after 2000 steps in above simulations), we consider w_i and w_f to be sufficiently close if $\|w_i - w_f\| < 0.0001$ and we consider the resulting periodic gait as a successful test in this evaluation. The threshold, 0.0001, is also chosen experimentally based on data histogram to consider two states identical at steady state, since obtaining true identical results (corresponds to threshold value of 0) would not be possible in numeric analysis. Table 6 illustrates the performance of three models on rough terrains, giving the percentage of successful runs in the sense mentioned above. As seen in Table 6, the MD-SLIP model has a better performance in converging to the initial apex state as compared to SLIP and TD-SLIP models.

Table 6 Percentage of the data points that are accepted as fixed point periodic gaits

Terrain	Model		
	SLIP	TD-SLIP	MD-SLIP
1	22.08	17.80	**95.18**
2	14.52	16.69	**78.74**
3	8.86	15.16	**62.42**
4	9.07	17.16	**79.50**
5	4.20	16.21	**63.79**
6	15.85	17.09	**84.16**
7	10.21	16.16	**74.00**

As can be seen from these simulations given in Tables 4, 5 and 6, the MD-SLIP model outperforms the other models in these tests, which allows us to observe that the periodic gait behavior of our model is sufficiently robust.

5.2 Closed-loop control with a deadbeat control strategy

This section investigates the performances of the three models for apex trajectory tracking under closed-loop control. We show that our proposed model yields better tracking performances with a deadbeat controller as compared to other two models.

In order to investigate our statement, we use numeric inverse of the apex return map as the controller in three models. The block diagram of the proposed deadbeat controller scheme is illustrated in Fig. 13. The inverse map controller takes desired apex state $w^d = (z_a^d, \dot{y}_a^d)$ and current apex state $w_i = (z_{ai}, \dot{y}_{ai})$ as input and cal-

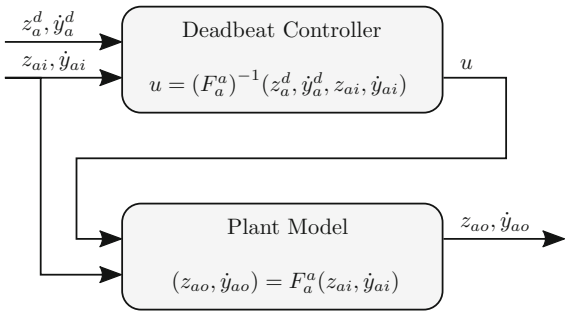

Fig. 13 Block diagram of the simple deadbeat controller used to compare the closed-loop performance of the models. Here u represents the generic controller output, which is different for different models. $(F_a^a)^{-1}$ is the inverse of the apex map and z_{ao}, $\dot{y}_{ao}$ are the apex height and apex horizontal velocity outputs, respectively

culates the control parameter u to achieve the desired apex state. Note that to have a fair comparison, we apply the same deadbeat controller for all three models. Here u represents the generic controller output, which is different for different models. For instance, in SLIP model, u refers to touchdown angle, θ_{td}, since it is the only control parameter. However, for TD-SLIP model, u represents both the touchdown angle, θ_{td}, and the constant touchdown parameter, α, that is used for determining torque applied to the hip. Finally, in MD-SLIP model, u refers to touchdown angle, θ_{td}, and constant control parameters C_0 and C_1.

Then the system uses this control parameter and achieves an apex state z_{ao}, $\dot{y}_{ao}$. This apex state is used as an input for the next cycle to compute the controller input for the next step.

We define different metrics to evaluate the tracking performance of the proposed closed-loop controller. The apex height tracking performance can be defined as

$$P_z = 100\sqrt{\frac{1}{n}\sum_{i=1}^{n}\left(\frac{z_{ai}-z_a^d}{z_a^d}\right)^2}, \tag{44}$$

where n is the total number of apexes, i is the apex index, z_{ai} is apex hight at ith index and z_a^d is the desired apex height. Similarly, apex horizontal velocity tracking performance can be defined as

$$P_{\dot{y}} = 100\sqrt{\frac{1}{n}\sum_{i=1}^{n}\left(\frac{\dot{y}_{ai}-\dot{y}_a^d}{\dot{y}_a^d}\right)^2}, \tag{45}$$

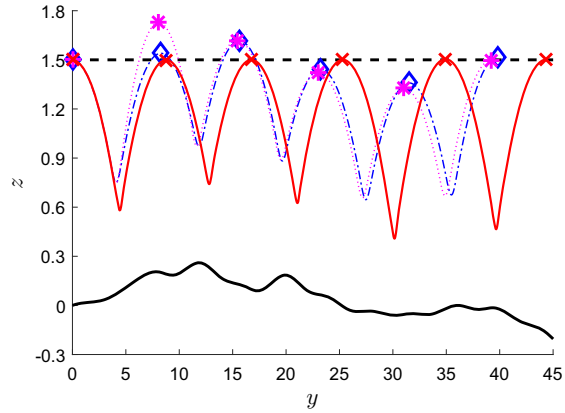

Fig. 14 During simulation terrain 3 is used and 5 steps are performed. Desired apex height 1.5 and desired apex speed 3.2 are simulated. *Black solid line* represents the ground. *Black dashed line* represents the desired apex height. *Blue* (*diamond*), *magenta* (*star*) and *red* (*cross*) points are the apex positions for SLIP, TD-SLIP and MD-SLIP models, respectively. *Blue* (*dot dashed*), *magenta* (*dotted*) and *red* (*solid*) *lines* are the trajectories that SLIP, TD-SLIP and MD-SLIP models follow, respectively. (Color figure online)

where $\dot{y}_{ai}$ is horizontal velocity at ith apex and $\dot{y}_a^d$ is the desired apex horizontal velocity.

Likewise, apex state tracking performance is defined as

$$P_a = 100\sqrt{\frac{1}{n}\sum_{i=1}^{n}\left(\frac{z_{ai}-z_a^d}{z_a^d}\right)^2 + \left(\frac{\dot{y}_{ai}-\dot{y}_a^d}{\dot{y}_a^d}\right)^2}. \tag{46}$$

Figure 14 illustrates a sample run of the three models running at terrain 3 with desired apex height 1.5 and desired apex speed 3.2. It can be clearly observed that MD-SLIP model and the associated closed-loop deadbeat controller preserves the desired apex states with a negligible error when compared to TD-SLIP and SLIP models. In order to generalize our results, we repeated this closed-loop control test for all 10000 initial conditions and computed the mean and standard deviations of the percentage tracking errors in (44), (45) and (46) for terrains 2–7. The results are listed in Table 7. Our results show that MD-SLIP model also outperforms the TD-SLIP and SLIP models when a basic closed-loop controller is used.

The quantities given by (44)–(46) obviously could be considered as measures to determine the locomotion performance. Indeed they indicate the deviations between the actual trajectory and the (desired) peri-

Table 7 Percentage tracking error of apex states in closed-loop system

Model and metric		Terrain					
		2	3	4	5	6	7
SLIP	P_z	0.694 ± 0.923	1.21 ± 1.58	0.724 ± 0.932	1.27 ± 1.58	0.409 ± 0.551	0.722 ± 0.965
	$P_{\dot{y}}$	0.229 ± 0.125	0.437 ± 0.224	0.267 ± 0.135	0.508 ± 0.246	0.138 ± 0.0719	0.256 ± 0.127
	P_a	0.771 ± 0.899	1.37 ± 1.53	0.826 ± 0.894	1.47 ± 1.51	0.460 ± 0.533	0.820 ± 0.928
TD-SLIP	P_z	1.31 ± 0.948	2.42 ± 1.60	1.40 ± 0.921	2.54 ± 1.53	0.779 ± 0.551	1.48 ± 0.967
	$P_{\dot{y}}$	1.36 ± 1.36	2.88 ± 2.75	1.72 ± 2.13	3.49 ± 4.23	0.870 ± 1.04	1.82 ± 2.11
	P_a	2.24 ± 1.12	4.41 ± 2.20	2.64 ± 1.82	5.08 ± 3.63	1.40 ± 0.894	2.76 ± 1.80
MD-SLIP	P_z	$\mathbf{0.107 \pm 0.115}$	$\mathbf{0.200 \pm 0.166}$	$\mathbf{0.122 \pm 0.154}$	$\mathbf{0.193 \pm 0.204}$	$\mathbf{0.0699 \pm 0.0874}$	$\mathbf{0.132 \pm 0.142}$
	$P_{\dot{y}}$	$\mathbf{0.171 \pm 0.0861}$	$\mathbf{0.350 \pm 0.168}$	$\mathbf{0.178 \pm 0.0886}$	$\mathbf{0.361 \pm 0.151}$	$\mathbf{0.0925 \pm 0.0484}$	$\mathbf{0.187 \pm 0.0838}$
	P_a	$\mathbf{0.215 \pm 0.122}$	$\mathbf{0.414 \pm 0.217}$	$\mathbf{0.241 \pm 0.143}$	$\mathbf{0.438 \pm 0.200}$	$\mathbf{0.128 \pm 0.0835}$	$\mathbf{0.246 \pm 0.139}$

odic gait during the locomotion over the rough terrains. Table 7 indicates that the MD-SLIP model with the proposed controller achieves better locomotion performance over rough terrains. Moreover, as indicated in [39], such mean–variance deviations could also be utilized as a measure for stability performance, or similarly for the robustness performance of the proposed controller. Hence, from this perspective, results given in Tables 4, 5, 6 and Table 7 are both supporting the conclusion that the MD-SLIP model not only yields better locomotion performance, but also has better stability robustness as compared to the other two SLIP templates.

6 Conclusion

In this paper, we considered a modification of well-known SLIP model, which is widely used for capturing and studying the running behavior in legged robots. Our modified model, which is called MD-SLIP, contains a linear (force) and a rotational (torque) actuator. By using partial feedback linearization technique, we propose control laws for the proposed actuators which are utilized in the stance phase. We show that with the proposed control laws, the MD-SLIP dynamics become integrable and we presented the analytical solutions to the controlled dynamics. By utilizing these solutions, we show that the controlled system possess stable periodic gaits for a large number of initial conditions. Then, through extensive simulations, we showed that the performance of MD-SLIP model with the proposed controllers is quite satisfactory and robust in rough terrains.

The following points maybe considered as the main contributions of the paper. We first introduced two actuators for the SLIP model. Then by using feedback linearization we proposed suitable control laws for these actuators. The resulting controlled dynamics become integrable, and the analytical solutions to these dynamics are given. These solutions are not arbitrary but are sufficiently similar to the actual locomotion trajectories generated by SLIP model. Moreover, by using these analytical solutions, at least theoretically, it is possible to obtain apex-to-apex mapping analytically. This mapping is important in determining the periodic gaits as well as their stability properties. We utilized this approach for symmetric gaits which indicates that the analytical results we obtained are sufficiently close to the ones obtained by simulation. By using our control parameters, it is possible to obtain asymmetrical and stable gaits. But investigating their stability properties analytically, although theoretically possible, is rather difficult due to highly nonlinear nature of the resulting expressions. For most of the cases, we resort to numerical solutions. Finally, we propose a feedback deadbeat controller which utilizes the inverse of the apex-to-apex map to determine and update the controller parameters to regulate the locomotion on different terrain profiles. We tested the performance of the proposed controller on several rough terrain profiles and our simulation results indicate that the proposed control law is quite satisfactory and yields a robust periodic gait behavior on rough terrains.

The results presented in this paper could be improved in various directions. Different control laws for linear and rotational actuators which yield integrable stance

dynamics could be developed and the performances of such control laws could be analyzed. The proposed control law could be utilized for motion planning due to its computational advantages (as a result of its analytic nature) as well as additional actuator in the proposed model supports adjusting leg placement for optimizing stability and energy efficiency for different terrains [25]. Finally, different feedback controllers could be pursued to regulate the running gaits on different terrains.

Acknoledgements Hasan Hamzaçebi was supported by Aselsan Inc. and The Scientific and Technological Research Council of Turkey (TÜBİTAK). The authors would like to thank İsmail Uyanık for his invaluable comments and suggestions.

References

1. Raibert, M.H.: Legged Robots that Balance. MIT Press, Cambridge (1986)
2. Holmes, P., Full, R.J., Koditschek, D., Guckenheimer, J.: The dynamics of legged locomotion: models, analyses, and challenges. SIAM Rev. **48**(2), 207–304 (2006)
3. Saranli, U., Buehler, M., Koditschek, D.E.: RHex: A simple and highly mobile robot. Int. J. Robot. Res. **20**(7), 616–631 (2001)
4. Dickinson, M.H., Farley, C.T., Full, R.J., Koehl, M.A.R., Kram, R., Lehman, S.: How animals move: an integrative view. Science **288**(5463), 100–106 (2000)
5. Fang, H., Li, S., Wang, K., Xu, J.: Phase coordination and phase-velocity relationship in metameric robot locomotion. Bioinspi. Biomim. **10**(6), 066006 (2015)
6. Wooden, D., Malchano, M., Blankespoor, K., Howardy, A., Rizzi, A.A., Raibert, M.: Autonomous navigation for BigDog. In: Proceedings of the 2010 IEEE International Conference on Robotics and Automation (ICRA), pp. 4736–4741 (2010)
7. Dubey, S., Prateek, M., Saxena, M.: Robot locomotion—a review. Int. J. Appl. Eng. Res. **10**(3), 7357–7369 (2015)
8. Kajita, S., Espiau, B.: Legged Robots. In: Siciliano, B., Khatib, O. (eds.) Springer Handbook of Robotics, pp. 361–389. Springer, Heidelberg (2008)
9. Saranlı, U., Arslan, Ö., Ankaralı, M.M., Morgül, Ö.: Approximate analytic solutions to non-symmetric stance trajectories of the passive spring-loaded inverted pendulum with damping. Nonlinear Dyn. **62**(4), 729–742 (2010)
10. Fang, H., Li, S., Wang, K.W., Xu, J.: A comprehensive study on the locomotion characteristics of a metameric earthworm-like robot; part a: modeling and gait generation. Multibody Syst. Dyn. **34**(4), 391–413 (2015)
11. Uyanik, I., Ankarali, M.M., Cowan, N.J., Saranli, U., Morgül, Ö.: Identification of a vertical hopping robot model via harmonic transfer functions. Trans. Inst. Meas. Control **38**(5), 501–511 (2016)
12. Pinto, C.M.: Stability of quadruped robots trajectories subjected to discrete perturbations. Nonlinear Dyn. **70**(3), 2089–2094 (2012)
13. Golubitsky, M., Stewart, I., Buono, P.L., Collins, J.: Symmetry in locomotor central pattern generators and animal gaits. Nature **401**(6754), 693–695 (1999)
14. Collins, J.J., Stewart, I.N.: Coupled nonlinear oscillators and the symmetries of animal gaits. J. Nonlinear Sci. **3**(1), 349–392 (1993)
15. Andrews, B., Miller, B., Schmitt, J., Clark, J.E.: Running over unknown rough terrain with a one-legged planar robot. Bioinspir. Biomim. **6**(2), 026009 (2011)
16. Blickhan, R., Full, R.J.: Similarity in multilegged locomotion: bouncing like a monopode. J. Comp. Physiol. A: Neuroethol., Sen., Neural, Behav. Physiol. **173**(5), 509–517 (1993)
17. Farley, C.T., Ferris, D.P.: Biomecahnics of walking and running: center of mass movements to muscle action. Excercise Sport Sci. Rev. **26**, 253–283 (1998)
18. Zeglin, G.: The bow leg hopping robot. Ph.D. thesis, Carnegie Mellon University, Pittsburgh, PA, USA (1999)
19. Hurst, J.W., Chestnutt, J.E., Rizzi, A.A.: Design and philosophy of the BiMASC, a highly dynamic biped. In: Proceedings of the 2007 IEEE International Conference on Robotics and Automation, pp. 1863–1868 (2007)
20. Ankarali, M.M., Saranli, U.: Stride-to-stride energy regulation for robust self-stability of a torque-actuated dissipative spring-mass hopper. Chaos: an Interdisciplinary. J. Nonlinear Sci. **20**(3), 033121 (2010)
21. Full, R.J., Koditschek, D.E.: Templates and anchors: neuromechanical hypotheses of legged locomotion on land. J. Exp. Biol. **202**(23), 3325–3332 (1999)
22. Han, B., Luo, X., Liu, Q., Zhou, B., Chen, X.: Hybrid control for SLIP-based robots running on unknown rough terrain. Robotica **32**(7), 1065–1080 (2014)
23. Schwind, W.J., Koditschek, D.E.: Approximating the stance map of a 2-DOF monoped runner. J. Nonlinear Sci. **10**(5), 533–568 (2000)
24. Holmes, P.: Poincaré, celestial mechanics, dynamical-systems theory and chaos. Phys. Rep. **193**(3), 137–163 (1990)
25. Arslan, Ö., Saranli, U.: Reactive planning and control of planar spring-mass running on rough terrain. IEEE Trans. Robot. **28**(3), 567–579 (2012)
26. Uyanik, I., Saranli, U., Morgül, Ö.: Adaptive control of a spring-mass hopper. In: Proceedings of the 2011 IEEE International Conference on Robotics and Automation (ICRA), pp. 2138–2143 (2011)
27. Geyer, H., Seyfarth, A., Blickhan, R.: Spring-mass running: simple approximate solution and application to gait stability. J. Theor. Biol. **232**(3), 315–328 (2005)
28. Uyanik, I., Morgül, Ö., Saranli, U.: Experimental validation of a feed-forward predictor for the spring-loaded inverted pendulum template. IEEE Trans. Robot. **31**(1), 208–216 (2015)
29. Piovan, G., Byl, K.: Enforced symmetry of the stance phase for the spring-loaded inverted pendulum. In: Proceedings of the 2012 IEEE International Conference on Robotics and Automation (ICRA), pp. 1908–1914 (2012)
30. Altendorfer, R., Saranli, U., Komsuoglu, H., Koditschek, D., Brown, H.B., Buehler, M., Moore, N., McMordie, D., Full, R.: Evidence for spring loaded inverted pendulum running in a hexapod robot. In: Rus, D., Singh, S. (eds.) Experimental Robotics VII, pp. 291–302. Springer, Heidelberg (2001)

31. Sato, A., Buehler, M.: A planar hopping robot with one actuator: design, simulation, and experimental results. In: Proceesings of the 2004 IEEE/RSJ International Conference on Intelligent Robots and Systems (IROS), pp. 3540–3545 (2004)
32. Poulakakis, I., Grizzle, J.W.: The spring loaded inverted pendulum as the hybrid zero dynamics of an asymmetric hopper. IEEE Trans. Autom. Control **54**(8), 1779–1793 (2009)
33. Secer, G., Saranli, U.: Control of hopping through active virtual tuning of leg damping for serially actuated legged robots. In: Proceedings of the 2014 IEEE International Conference on Robotics and Automation (ICRA), pp. 4556–4561 (2014)
34. Schmitt, J., Clark, J.: Modeling posture-dependent leg actuation in sagittal plane locomotion. Bioinspir. Biomim. **4**(4), 046005 (2009)
35. Peuker, F., Seyfarth, A., Grimmer, S.: Inheritance of SLIP running stability to a single-legged and bipedal model with leg mass and damping. In: Proceedings of the 2012 4th IEEE RAS & EMBS International Conference on Biomedical Robotics and Biomechatronics (BioRob), pp. 395–400 (2012)
36. Uyanik, I.: Adaptive control of a one-legged hopping robot through dynamically embedded spring-loaded inverted pendulum template. M.Sc. thesis, Bilkent University, Ankara, Turkey (2011)
37. Hamzaçebi, H., Morgül, Ö.: Enlarging the region of stability using the torque-enhanced active SLIP model. In: Proceedings of the 2015 IEEE International Conference on Advanced Robotics (ICAR), pp. 345–350 (2015)
38. Khalil, H.K.: Nonlinear Systems, 3rd edn. Prentice Hall, Upper Saddle River (2002)
39. Miller, B., Schmitt, J., Clark, J.E.: Quantifying disturbance rejection of SLIP-like running systems. Int. J. Robot. Res. **31**(5), 573–587 (2012)
40. Welch, P.D.: The use of fast fourier transform for the estimation of power spectra: a method based on time averaging over short, modified periodograms. IEEE Trans. Audio Electroacoust. **15**(2), 70–73 (1967)